Jurnal Teknologi

Full Paper

CFD INVESTIGATION OF WIND-STRUCTURE INTERACTIONS IN DENSE URBAN ENVIRONMENT: EFFECTS OF SPACING BETWEEN BUILDINGS

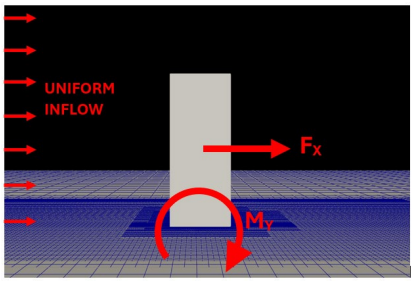
Mohamad Hasif Osman[a]*, Azlan Adnan[a], Adibah Fatihah Mohd Yusof[b], Noram Irwan Ramli[c]

[a]Faculty of Civil Engineering, Universiti Teknologi Malaysia, 81310 UTM Johor Bahru, Johor, Malaysia
[b]Faculty of Mechanical Engineering, Universiti Teknologi Malaysia, 81310 UTM Johor Bahru, Johor, Malaysia
[c]Faculty of Civil Engineering Technology, Universiti Malaysia Pahang Al-Sultan Abdullah, 26300 Kuantan, Pahang, Malaysia

Article history
Received
3rd September 2025
Received in revised form
17th December 2025
Accepted
22nd December 2025
Published
1st November 2026

*Corresponding author
mohamad.hasif@utm.my

Graphical abstract



Abstract

Dense urban developments with closely spaced high-rise buildings create complex wind–structure interactions that are not fully captured by existing studies, which often focus on isolated buildings or lack rigorous mesh optimisation and validation; this study addresses that gap by systematically examining how inter-building spacing modifies wind-induced pressures and velocity fields. The aim is to establish a validated, computationally efficient CFD framework for multi-building interference, with specific objectives to: (i) quantify the effects of spacing on windward pressures and suction zones under both uniform and atmospheric boundary layer inflows, and (ii) optimise a mesh and turbulence-modelling strategy that is suitable for routine engineering design workflows. The present study uses validated Reynolds-Averaged Navier–Stokes (RANS) simulations with a standard k–epsilon model under both uniform and atmospheric boundary layer inflows. A mesh sensitivity analysis identifies an optimal grid of 1.7 million cells and validation against CAARC wind tunnel data shows close agreement in ABL profiles and peak pressure coefficients on windward faces. Despite its simplicity, the standard k–epsilon closure is adopted as a practical engineering choice because, for tall-building cases, it reproduces time-averaged pressures and moments comparable to more advanced models but at far lower computational cost, enabling parametric studies across multiple spacing configurations. Reducing spacing from 250 m to 50 m increases peak windward pressures on the downstream taller building by approximately 8% near the top and amplifies minimum suction near the base by up to 60%, with local pressure magnitudes reaching 0.50 kPa and producing up to 20% higher base moments about the y-axis than at the widest spacing. Vertical pressure profiles show that lower façade regions are most sensitive to spacing, with shifts in the height of extreme suction and noticeable asymmetry between left and right façades due to the upstream building's slight plan offset. These findings demonstrate that carefully resolved, validated k–epsilon-based RANS can capture critical interference effects and yield spacing-dependent design metrics, underscoring the need for façade-specific wind load mitigation to improve wind resilience in dense urban environments.

Keywords: Atmospheric Boundary Layer (ABL), Building interference, Computation Fluid Dynamics (CFD), Urban aerodynamics, Wind load

DOI: https://doi.org/10.11113/jurnalteknologi.v89.25538

Abstrak

Pembangunan bandar berketumpatan tinggi dengan bangunan tinggi yang tersusun rapat mewujudkan interaksi angin–struktur yang kompleks yang tidak sepenuhnya ditangani oleh kajian sedia ada, yang lazimnya menumpukan kepada bangunan terasing atau kurang dari segi pengoptimuman jejaring dan pengesahan yang rapi; kajian ini menangani jurang tersebut dengan meneliti secara sistematik bagaimana jarak antara bangunan mengubah tekanan akibat angin dan medan halaju. Tujuan kajian ini adalah untuk mewujudkan rangka kerja CFD yang disahkan dan cekap dari segi pengiraan bagi analisis gangguan antara berbilang bangunan, dengan objektif khusus untuk: (i) mengkuantifikasikan kesan jarak terhadap tekanan angin hadapan dan zon sedutan di bawah keadaan aliran seragam dan lapisan sempadan atmosfera, dan (ii) mengoptimumkan strategi jejaring dan pemodelan pergolakan yang sesuai untuk aliran kerja reka bentuk kejuruteraan rutin. Kajian ini menggunakan simulasi Reynolds-Averaged Navier–Stokes (RANS) yang telah disahkan dengan model k–epsilon piawai di bawah aliran seragam dan lapisan sempadan atmosfera. Analisis sensitiviti jejaring mengenal pasti grid optimum sebanyak 1.7 juta sel dan pengesahan terhadap data terowong angin CAARC menunjukkan persetujuan yang baik bagi profil ABL dan pekali tekanan puncak pada permukaan angin hadapan. Walaupun bersifat ringkas, penutupan k–epsilon piawai dipilih sebagai pilihan kejuruteraan yang praktikal kerana, bagi kes bangunan tinggi, ia menghasilkan tekanan dan momen purata masa yang setara dengan model yang lebih maju tetapi pada kos pengiraan yang jauh lebih rendah, sekali gus membolehkan kajian parametrik merentasi pelbagai konfigurasi jarak. Pengurangan jarak daripada 250 m kepada 50 m meningkatkan tekanan puncak pada bahagian angin bangunan hilir yang lebih tinggi kira-kira 8% berhampiran bahagian atas dan menguatkan sedutan minimum berhampiran dasar sehingga 60%, dengan magnitud tekanan setempat mencecah 0.50 kPa dan menghasilkan sehingga 20% peningkatan momen dasar tentang paksi-y berbanding jarak paling luas. Profil tekanan menegak menunjukkan bahawa zon fasad bahagian bawah adalah paling sensitif terhadap jarak, dengan peralihan pada ketinggian sedutan ekstrem dan ketaksimetrian yang ketara antara fasad kiri dan kanan akibat sedikit anjakan pelan bangunan hulu. Penemuan ini menunjukkan bahawa RANS berasaskan k–epsilon yang diselesaikan dengan teliti dan disahkan boleh menangkap kesan gangguan kritikal dan menghasilkan metrik reka bentuk yang bergantung kepada jarak, sekali gus menekankan keperluan mitigasi beban angin khusus fasad bagi meningkatkan ketahanan angin dalam persekitaran bandar berketumpatan tinggi.

©2026 Penerbit UTM Press. All rights reserved

1.0 INTRODUCTION

Urban wind engineering faces escalating challenges as cities increasingly adopt dense, vertically oriented architectures that amplify aerodynamic complexities and wind-structure interactions. Computational fluid dynamics (CFD) has become indispensable for evaluating wind loads, pressure distributions, and flow patterns around high-rise structures, particularly where wind tunnel testing proves logistically constrained or cost-prohibitive [1,12]. While advancements in turbulence modelling and grid generation techniques have enhanced simulation fidelity, critical knowledge gaps persist regarding the interplay between mesh resolution, validation protocols, and interference effects in multi-building configurations [5,17]. Existing studies predominantly focus on isolated structures or simplified urban layouts, inadequately addressing the three-dimensional flow modifications induced by variable building spacings and oblique wind angles in real-world settings [2,13].

Recent advancements continue to emphasize the crucial impact of building layout on urban wind flow and pedestrian comfort. Cui et al. [6] demonstrated that increasing the spacing ratio among high-rise buildings lowers mutual aerodynamic interference, thereby enhancing the pedestrian-level wind environment, especially in unique clustered layouts. Complementing this, Mon Soe et al. [15] used CFD to reveal that variable building orientation and proximity significantly modulate localized wind speeds and pressure distributions within urban building clusters, directly affecting both structural loading and microclimate at ground level. These studies further underline the necessity for parametric CFD analyses in high-density urban planning, where both wind comfort and safety must be simultaneously addressed.

DOI: https://doi.org/10.11113/jurnalteknologi.v89.25538

The accuracy of CFD predictions hinges on rigorous mesh sensitivity analyses, as suboptimal grid densities may overestimate peak pressures by 15-20% or misrepresent separation zones, compromising structural reliability [7,8]. Furthermore, validation studies often neglect the compounding effects of atmospheric boundary layer (ABL) shear and transitional turbulence regimes, leading to discrepancies in predicting suction pressures at building bases and corners [10,15]. Previous work by Li et al. [9] and Reiter [17] underscores the necessity of integrating advanced turbulence closures like transitional SST k-ω models to capture flow separation dynamics, yet their application remains limited in practical engineering workflows. Although Tominaga and Stathopoulos [19] and Shirzadi et al. [18] demonstrate that even though Steady Reynolds Averaged Navier-Stokes (SRANS) has contributed most in the field of wind engineering, they are still far from accurate when compared to the experimental results. They proved that Large Eddy Simulation (LES) produces better accuracy compared to SRANS, in terms of modelling both isolated and group buildings. However, when analysing the time-averaged results, LES shows almost similar results to SRANS, especially the standard k-epsilon model [18].

The literature reveals that existing studies largely focus on isolated buildings or simplified urban layouts, insufficiently capturing the multi-dimensional flow interactions affected by variations in building spacing, while mesh sensitivity and validation efforts often remain inadequate, potentially causing overestimation of peak pressures [3, 5, 7]. Furthermore, the complex effects of atmospheric boundary layer shear, transitional turbulence, and dynamic urban wind phenomena like wake vortices' impact on adjacent buildings are insufficiently integrated in current research [13, 15]. The present study bridges these gaps by conducting systematically validated RANS simulations with mesh optimization in OpenFOAM to assess the aerodynamic interference between adjacent high-rise buildings under realistic atmospheric boundary layer conditions and varied spacing. This approach enables detailed insights into localized pressure distributions and structural moments [9, 10, 11].

This study aims to systematically investigate the aerodynamic interdependence between adjacent high-rise buildings across three critical dimensions: (1) quantifying the influence of inter-building spacing on windward pressure distributions, velocity fields, and structural moments under uniform and sheared ABL inflows; and (2) establishing validated CFD protocols that reconcile mesh optimisation strategies from Blocken et al. [3] with experimental benchmarks from CAARC standard model tests by Li et al. [9].

2.0 METHODOLOGY

2.1 Numerical Model

The Reynolds-Averaged Navier-Stokes (RANS) equations are widely used in computational fluid dynamics (CFD) for simulating turbulent flows [16]. When coupled with the k-epsilon (k-ε) turbulence model, they provide a robust framework for modelling incompressible, steady-state flows [18]. This combination is particularly effective in OpenFOAM, a robust open-source CFD code.

For incompressible flows, the density is assumed constant, simplifying the RANS equations.
Continuity Equation:

$$\frac{\partial u_i}{\partial x_i} = 0 \tag{1}$$

Momentum Equation:

$$u_j \frac{\partial u_i}{\partial x_j} = -\frac{1}{\rho}\frac{\partial p}{\partial x_i} + v\frac{\partial^2 u_i}{\partial x_j^2} - \frac{\partial \overline{u_i' u_j'}}{\partial x_j} \tag{2}$$

Here, u_i is the mean velocity component, p is the pressure, ρ is the fluid density, v is the kinematic viscosity, and $\overline{u_i' u_j'}$ represents the Reynolds stress tensor.

The present study uses the standard k-epsilon model to close the Navier-Stokes The choice of the k-epsilon turbulence model in this study is justified by its widespread use and proven reliability in simulating turbulent flows around buildings in urban wind engineering. The k-epsilon model can effectively capture key flow features such as recirculation zones, shear layers, and pressure distributions on building surfaces, striking a practical balance between accuracy and computational cost essential for large-scale CFD studies involving multiple building configurations [17, 18, 19]. Although more advanced models like Large Eddy Simulation (LES) can provide higher accuracy in capturing unsteady and complex turbulence phenomena, their high computational demand makes them less feasible for parametric urban wind flow investigations [18]. Given these considerations, the k-epsilon model remains an appropriate and efficient choice for this research's objectives.

The k-epsilon model solves two transport equations: one for the turbulent kinetic energy (k) and another for the dissipation rate of turbulent kinetic energy (ε). These equations are used to calculate the turbulent viscosity (μt), which models the Reynolds stresses [20].

DOI: https://doi.org/10.11113/jurnalteknologi.v89.25538

The computational setup for the present study employed a steady-state simulation with 7000 to 10,000 iterations to ensure solution convergence. Boundary conditions included a velocity inlet for the inflow, prescribing the fluid entry velocity, and a zero gradient condition at the outlet, allowing the flow to exit smoothly by setting the gradient of flow variables to zero. The side walls, ground, and building surfaces were assigned zero gradient conditions, implying no flux across these boundaries and extrapolating interior values to the boundaries. The top boundary was set to atmospheric conditions, imposing a fixed pressure representative of the ambient environment. This configuration facilitated a stable and computationally efficient solution for the incompressible flow scenario [11, 18]. The summary of each boundary condition is given in Table 1 below.

Table 1 Minimum cell sizes for four different meshes in the x, y, and z directions of the Cartesian coordinate system

Boundary Name	Boundary Condition Type	Description
Inlet	Velocity Inlet	Prescribed uniform or ABL profile
Outlet	Zero Gradient	Flow variables gradient zeroed
Side Walls	Symmetry / Zero Gradient	No flux across boundaries
Ground	No Slip Wall	Zero velocity at surfaces
Buildings	No Slip Wall	Zero velocity at surfaces
Top	Fixed Pressure	Atmospheric pressure

2.2 Mesh Sensitivity Study

The mesh sensitivity analysis reveals critical insights into grid resolution requirements for accurate CFD simulations of wind loads on tall buildings. Figure 1 shows the computational domain for the mesh sensitivity study, using only a single building. Table 2 shows the minimum cell sizes around the building surface and the total number of cells in each mesh. As demonstrated in Figure 3, horizontal force (FX) and base moment (MY) values (refer to Figure 2 for the definition of FX and MY) vary by 15-20% between Mesh 1 (coarsest) and Mesh 4 (finest), with convergence achieved at Mesh 3 (1.7 million cells). This aligns with validation guidelines from Reiter [17], who emphasized grid resolution optimization through systematic comparisons with wind tunnel data, particularly near building surfaces where pressure gradients are steep. The selected Mesh 3 balances computational efficiency with accuracy, mirroring strategies in urban wind flow studies where excessive mesh density showed diminishing returns for pressure prediction [15].

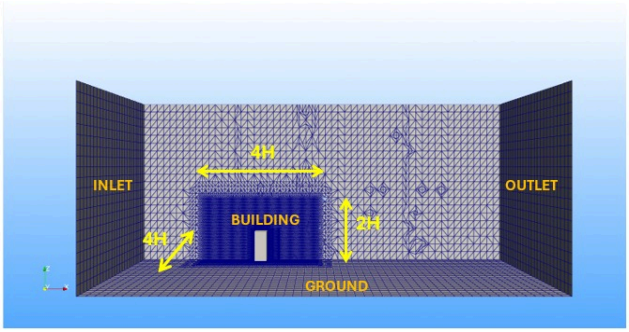


Figure 1 Computational domain for the mesh sensitivity study, using only a single building, with height H = 75m, located 4H downstream from the inlet boundary. The refinement box surrounding the building has a dimension of 4H (x-dir.) x 4H (y-dir.) x 2H (z-dir.), with the building located at the centre of the refinement box region.

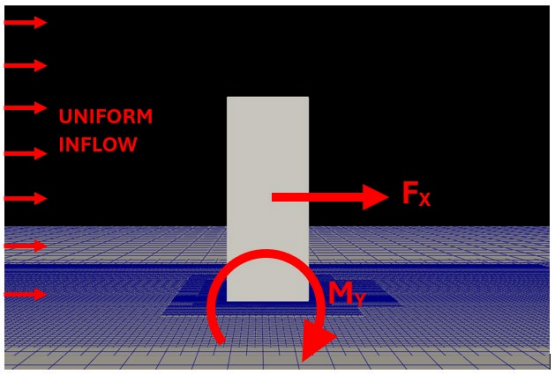


Figure. 2 Definition of horizontal force F_X and moment about the y-axis, M_Y of the centroid of the building's ground floor, simulated under a uniform flow with wind velocity of 30 m/s

Table 2 Minimum cell sizes for four different meshes in the x, y, and z directions of the Cartesian coordinate system. The final row shows the total number of cells inside the entire domain for each mesh.

Mesh	1	2	3	4
Cell size x [m]	0.517	0.259	0.129	0.065
Cell size y [m]	0.563	0.281	0.141	0.070
Cell size z [m]	0.625	0.313	0.156	0.078
Mesh volume [x10^6]	2.977	4.253	6.076	8.680

3.0 RESULTS AND DISCUSSION

3.1 Model Validation

Validation against Li et al. [9] wind tunnel experiments demonstrate strong agreement in both atmospheric boundary layer (ABL) profiles (R^2>0.98) and surface pressure coefficients at 2/3 building height (Figures 5-6). Figure 4 shows the computational domain model and physical model from Li et al. [9] of the CAARC standard tall building model. Although over-predicted compared to the

DOI: https://doi.org/10.11113/jurnalteknologi.v89.25538

wind tunnel experiment result, the pressure coefficient distribution of the present study shows good agreement with maximum positive values of C_p = 1.0 on windward faces and negative values reaching -0.8 at separation (suction) zones [15], consistent with patterns observed in CFD validation studies of single-building configurations [17].

The study could be enhanced by implementing transitional *k-ω* SST turbulence models, which Reiter [17] found essential for capturing flow separation details in building aerodynamics. While the current atmospheric boundary layer (ABL) simulation matches wind tunnel velocity profiles (as shown in Figure 5), recent research highlights the need to consider downburst wind effects in dense urban areas, as these can generate 12-15% higher negative pressures than traditional ABL flows [14,15]. Future work should integrate dynamic mesh adaptation techniques to resolve localized vortices identified in building wake regions [15,17], particularly emphasizing crosswind excitation analysis in tall structure design.

3.2 Varies Distance Between two Buildings

The plan view of the buildings is shown in Figure 7, where the distance L, representing the distance from the inlet to the first building (yellow-coloured), remains constant at 300 meters, while the distance x, which is the spacing between the yellow and red-coloured buildings, varies and takes values of 50, 150, and 250 meters. The incoming wind flow angle is 0°. The present study adopts the building arrangements from Eurocode 1 [4], as shown in Figure 7a, where H_{low} = 30m, H_{high} = 75m, H_{avg} = 30m, d_{large} = 50m and d_{small} = 15m. However, the present study changes the arrangement slightly, where all buildings are in the same orientation (0° from incoming wind angle, unless otherwise specified).

3.3 Uniform Flow Case

Figure 8 presents a comparison of windward pressure distributions on the first and tallest buildings for each spacing scenario. In this section, only uniform flow distribution (non-sheared flow) is considered. The purpose is to investigate the uninterrupted inflow without the roughness effect from the ground level. The results indicate that at the closest spacing of 50 meters, the tallest building experiences notably higher windward pressures than the upstream building, with the difference diminishing as the spacing increases to 250 meters. This trend highlights the pronounced interference effect at close proximities, where the downstream building is subjected to intensified wind loads due to the channeling and acceleration of flow between the structures. As the inter-building distance increases, the pressure difference becomes less significant, suggesting a transition toward isolated building behavior.

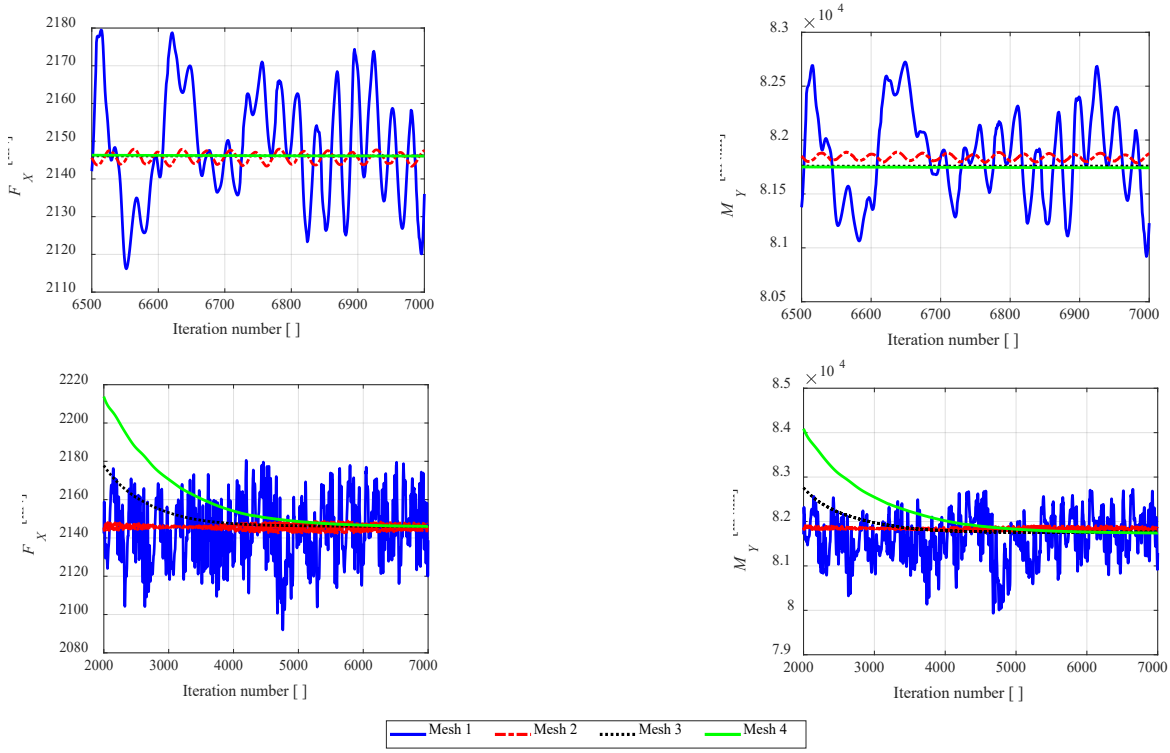
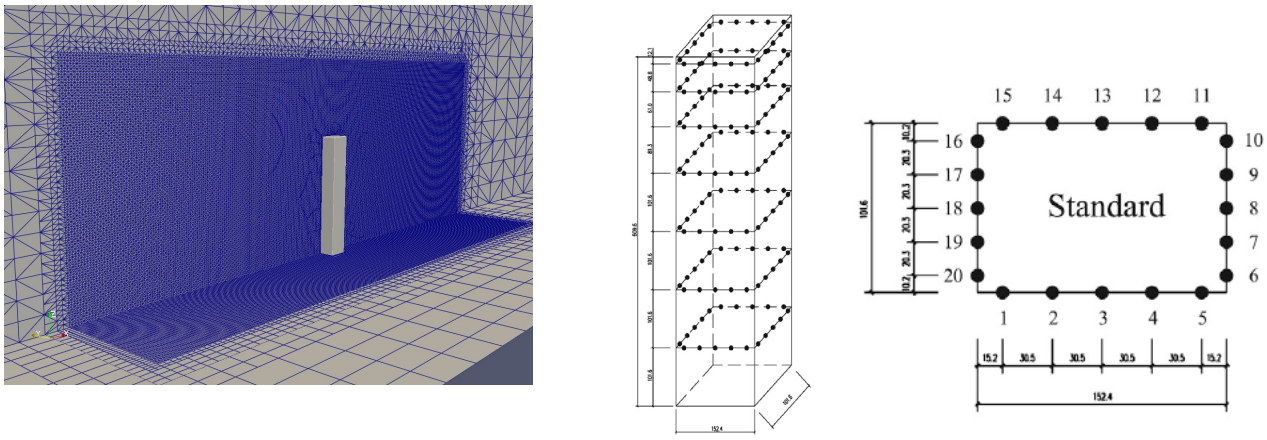


Figure 3 Comparison between all meshes for the FX and MY, where significant variation exists between the coarsest and finest mesh used in the present study. Mesh 3 is chosen for the present study to minimise computational costs while maintaining simulation accuracy

DOI: https://doi.org/10.11113/jurnalteknologi.v89.25538



(a) (b)

Figure 4 Computational domain (a) of the CAARC standard tall building model. The physical model (b) used in the experiment by Li et al. [9], where the numbering of pressure sensors (sensors 1 to 20) is shown in the figure.

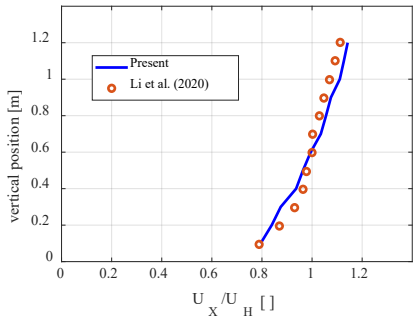


Figure 5 Atmospheric boundary layer model validation with experimental result from Li et al. [9].

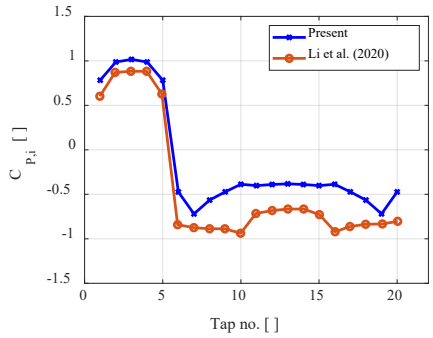
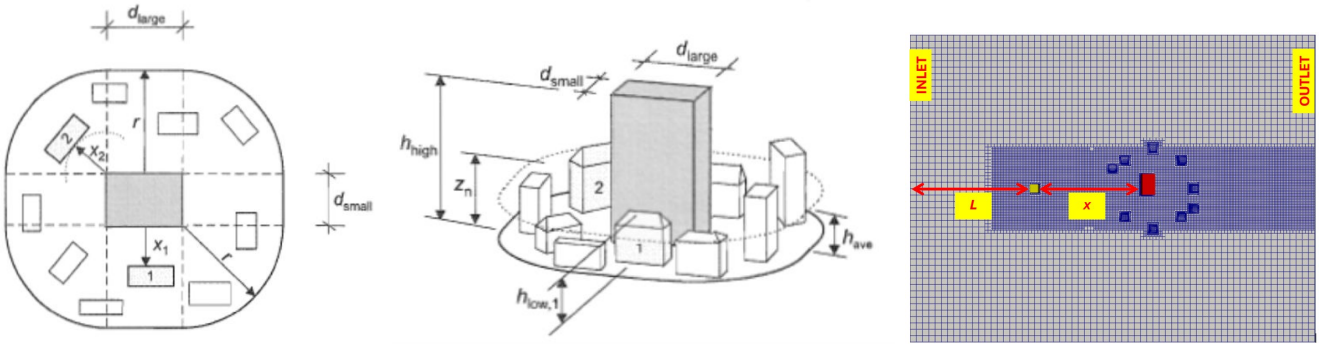


Figure 6 The pressure coefficient at 2/3 height of the CAARC standard tall building model was validated against experimental results from Li et al. [9].



(a) (b)

Figure 7 (a) Building arrangements based on Eurocode 1 [4] that was adopted in the present study, where H_{low} = 30m, H_{high} = 75m, H_{avg} = 30m, d_{large} = 50m and d_{small} = 15m; (b)the plan view of the buildings. The distance *L* is the distance from the inlet to the first building (Yellow colour). The distance between the Yellow and Red colored buildings varies in x = 50, 150, and 250m

DOI: https://doi.org/10.11113/jurnalteknologi.v89.25538

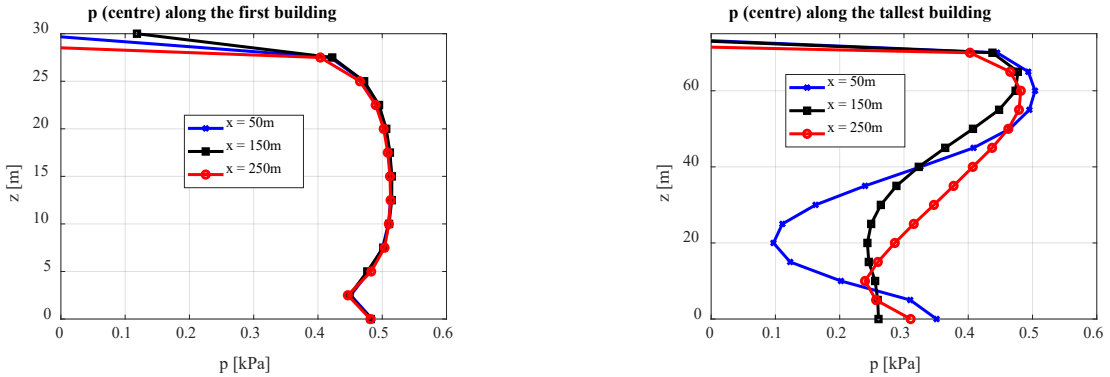
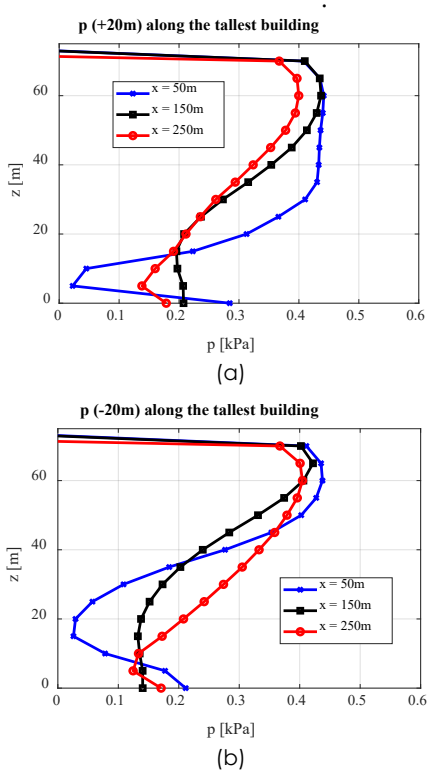


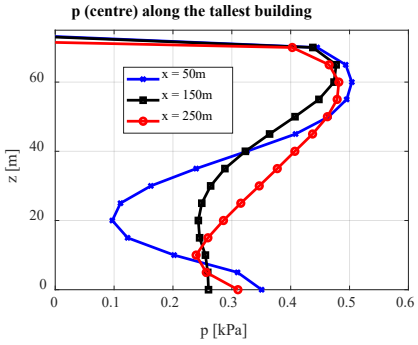
Figure 8 Pressure distribution (on the windward side of the building) comparison between (a) the first and (b) tallest buildings, at various distance x

Further insights are provided by Figure 9, which details the windward pressure distribution at the tallest building, measured at the centerline, left, and right sides. At the smallest spacing, the centerline records the highest pressures, while the lateral positions show slightly reduced values. This three-dimensional variation in pressure distribution underscores the complexity of the flow field, especially when buildings are closely spaced. The disparity in pressures across the building face is indicative of strong flow separation and localized acceleration effects, which are well-documented phenomena in both wind tunnel and CFD studies of urban environments [11,15].

Figure 10 offers a visual representation of the pressure field on the building surfaces for the 50-meter and 250-meter spacing cases. At the closer spacing, the pressure field on the windward side is more concentrated and intense, while the pressure distribution becomes more uniform and less severe as the spacing increases. These observations are consistent with established findings in urban wind load research, where closely spaced buildings exhibit more pronounced pressure gradients due to restricted flow paths and increased turbulence

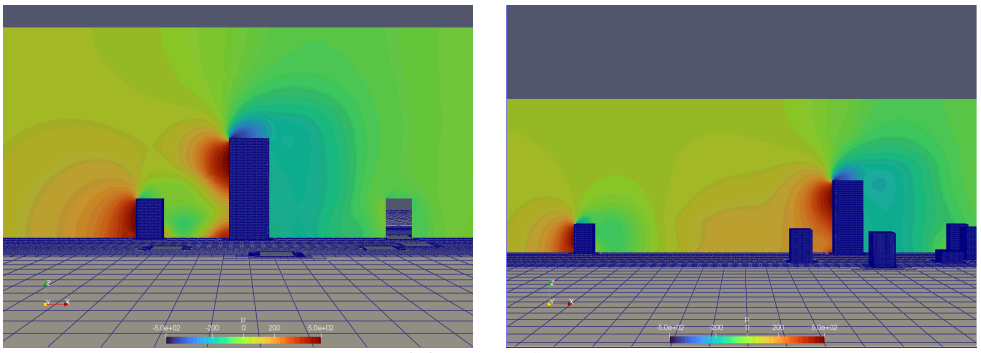


DOI: https://doi.org/10.11113/jurnalteknologi.v89.25538

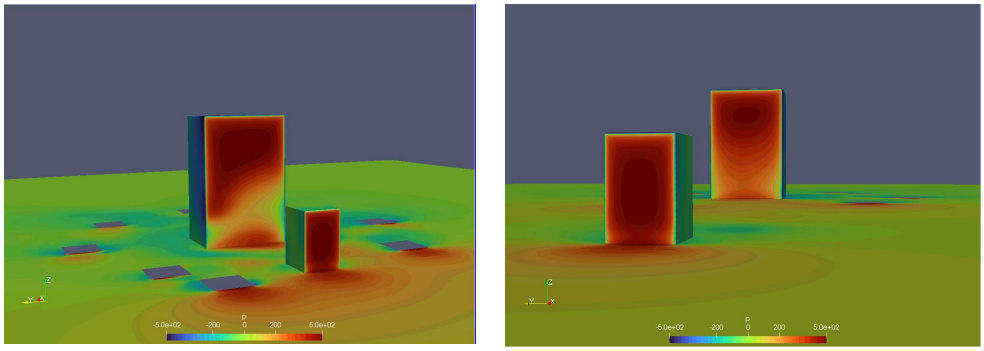


(c)

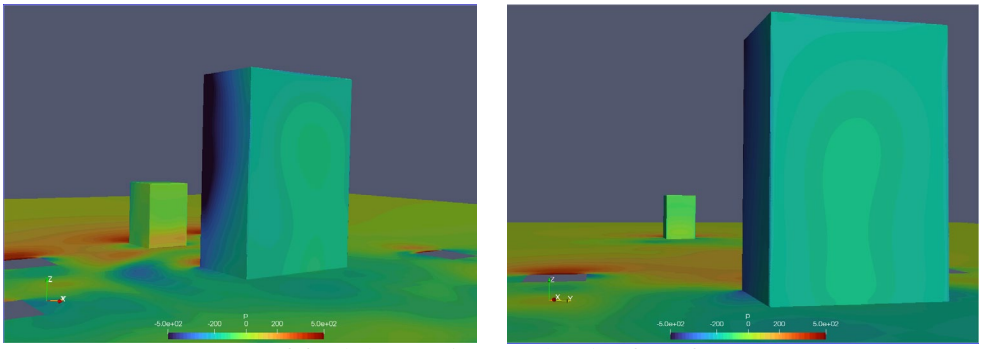
Figure 9 Pressure distribution (on the windward side of the building) at the tallest building, probed at the (a) left side, (b) right-side and (c) centerline of the building, at various distance x



(a) Pressure field



(b) Buildings' surface pressure side (front)



(c) Buildings' surface suction side (back)

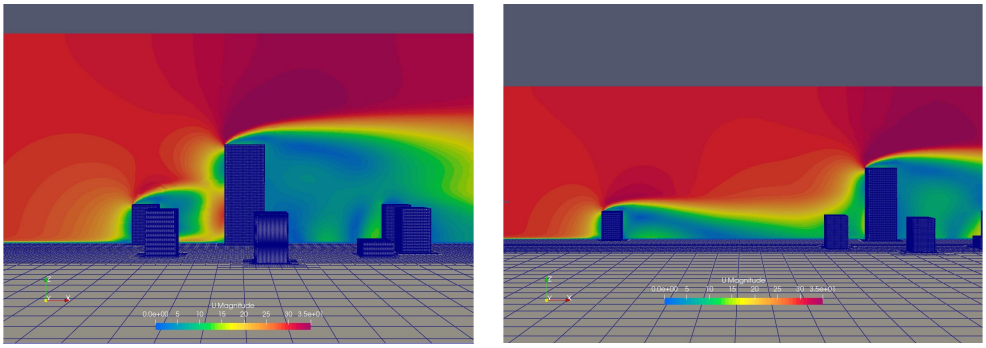
Figure 10 Pressure distribution (in the unit Pa) for distance x = 50m (left) and 250m (right)

DOI: https://doi.org/10.11113/jurnalteknologi.v89.25538

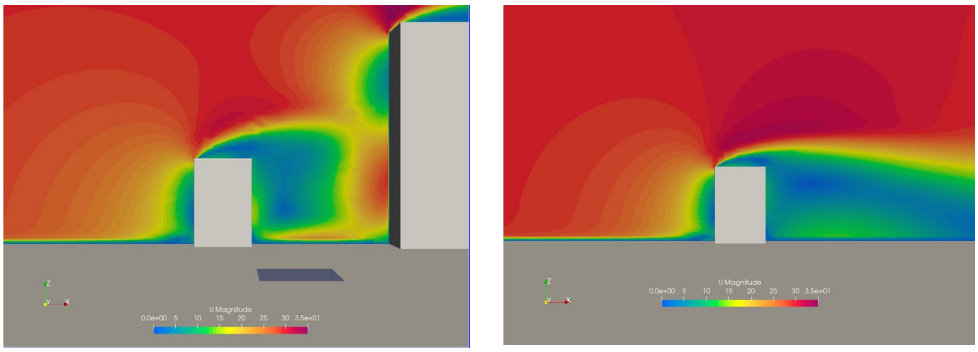
The velocity field distributions shown in Figure 11 further reinforce these findings. For the 50-meter spacing, there is a marked acceleration of flow between the buildings, with velocity magnitudes significantly exceeding those observed at greater spacings. This accelerated flow not only contributes to the higher windward pressures on the tallest building but also leads to more complex wake structures and recirculation zones downstream. At 250 meters, the velocity field is more dispersed, and the wake regions are broader and less intense, reflecting the reduced interaction between the buildings.

Structural response to these aerodynamic loads is quantified in Figure 12, which depicts the moment of the y-axis for both the first and tallest buildings across all spacing scenarios. The tallest building at 50-meter spacing experiences the highest moment, a direct consequence of the elevated windward pressures and intensified flow interaction. As the spacing increases, the moment values for both buildings converge, indicating a reduction in interference effects and a shift toward independent load response.

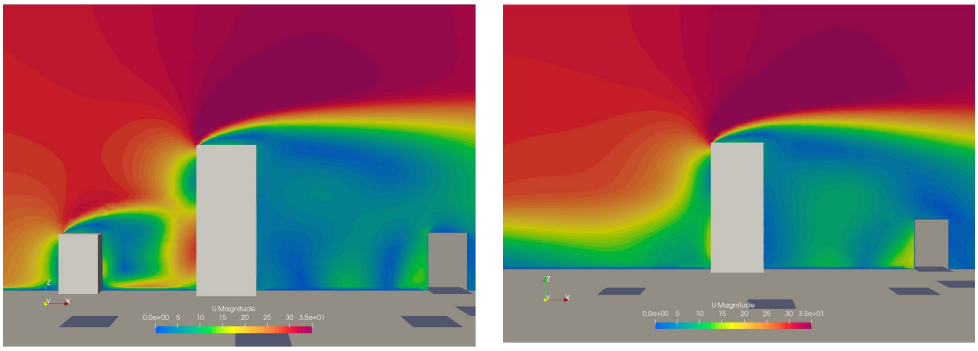
Overall, the data clearly demonstrate that building spacing plays a critical role in determining wind-induced pressures, velocity distributions, and structural moments in urban environments. Closely spaced buildings experience stronger aerodynamic interactions, leading to higher localized pressures and greater structural demands. These findings are consistent with established literature on wind around buildings, wind tunnel studies, and CFD analyses for urban wind load assessment, emphasizing the need for careful consideration of building arrangement in urban planning and design.



(a) Velocity field



(b) Velocity field at the first building



(c) Velocity field at the tallest building

Figure 11 Velocity (magnitude, in the unit m/s)) distribution for distance x = 50m (left) and 250m (right)

DOI: https://doi.org/10.11113/jurnalteknologi.v89.25538

3.4 Atmospheric Boundary Layer (Sheared Flow) Case

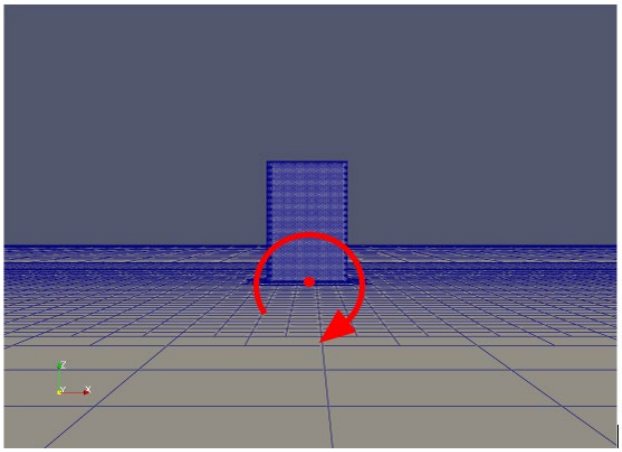
The present model validated the ABL profile with the result from [9] and is given in Figure 5, while the pressure distribution validation result for the standard CAARC tall building in ABL wind profile condition is presented in Figure 6. The pressure distribution along the vertical direction at the centerline of the first (yellow) building, as shown in Figure 13, is analyzed for three horizontal distances: x = 50m, 150m, and 250m, with the vertical distance normalized by the building's height of 30m. The maximum pressure of $p_{\max}$ =0.376 *kPa* occurs at at z=22.5 *m* for x=250 m, while $p_{\max}$ =0.363 *kPa* is observed at the same height (z=22.5 m) for =50 m, resulting in a 3.5% difference between the two values. Conversely, the minimum pressure of $p_{\min}$ =0.259 *kPa* occurs at z=5 m for both x=50 m and x=250 m, showing no percentage difference (0%) and consistent vertical positioning across these configurations.

The pressure distribution along the vertical direction at the centerline of the tallest (red) building, as shown in Fig. 14, is analyzed for three horizontal distances: x = 50m, 150m, and 250m, with the vertical distance normalized by the building's height of 75m. The maximum pressure of $p_{\max}$ =0.471*kPa* occurs at z=65 m for x=250 m, while $p_{\max}$ =0.497*kPa* is observed at the same height (z=65 m) for x=50 m, resulting in a 5.4% difference between the two values. Both $p_{\max}$ values occur at z=65 m (normalized height: 65/75≈0.87), suggesting consistent high-pressure zones near the building's top. The small magnitude difference (5.4%) implies minor sensitivity to horizontal spacing in upper regions.

In contrast, minimum pressure values differ significantly: $p_{\min}$ =0.218 *kPa* at z=10 m (x=250 m) and $p_{\min}$ =0.14*kPa* at z=15 m (x=50 m), resulting in a 43.6% magnitude difference and a 5m vertical positional shift. The 43.6% difference in $p_{\max}$ and the 5m vertical shift highlights strong sensitivity to horizontal distance (x) in lower regions of the building. Normalized vertical positions (z = 10/75 ≈ 0.13 vs. 15/75 = 0.2) suggest ground effects or vortex shedding patterns change with building spacing.

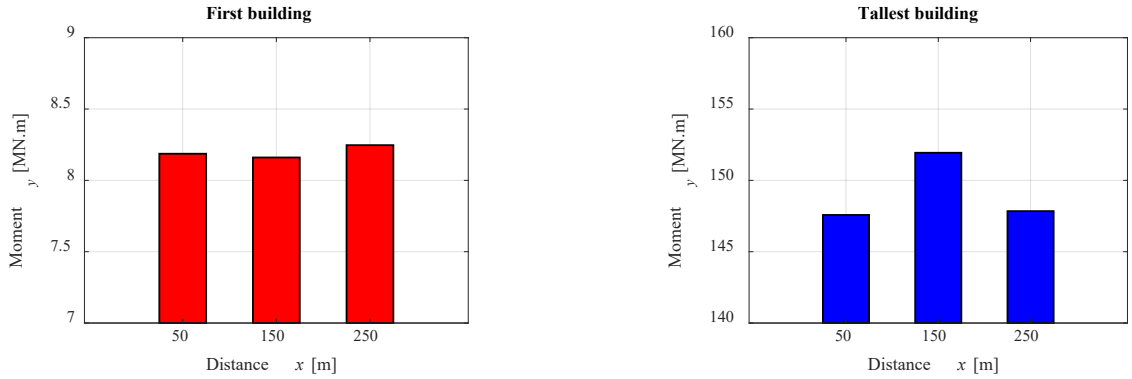
The vertical pressure distribution 20 meters left of the centerline on the tallest (red) building, as shown in Figure 15, is examined for horizontal distances of x = 50m, 150m, 250m, with vertical distances normalized by the building's height of 75m. Maximum pressure values are $p_{\max}$ =0.428 kPa at z=70 m (x=250 m) and $p_{\max}$ =0.449 *kPa* at the same height (x=50 m), showing a 4.8% difference in magnitude at identical vertical positions. Both $p_{\max}$ values occur at z=70 m (normalized height: 70/75 ≈ 0.93), indicating consistent high-pressure zones near the building's apex, likely due to accelerated airflow at the top. The small magnitude difference (4.8%) suggests minimal impact from horizontal spacing on peak pressures at elevated positions.

Minimum pressure values, however, differ more sharply: $p_{\min}$ =0.086*kPa* at z=5 m (x=250 m) and $p_{\min}$ =0.072 *kPa* at z=10 m (x=50 m), resulting in a 17.7% magnitude difference and a 5m vertical positional shift. The 17.7% difference in $p_{\min}$ and the 5m vertical shift reveals significant sensitivity to horizontal spacing near the building's base. At x=50 m, the lower pressure (0.072*kPa*) occurs higher up (z=10 m vs. 5 m), suggesting closer spacing may alter ground-level vortex dynamics or boundary layer separation.



(a) Moment about the y-axis (i.e., the wind flows in the x-direction), where the COR is at the centre-bottom of the building.

DOI: https://doi.org/10.11113/jurnalteknologi.v89.25538



(b) Moment about the y-axis (in Mega Newton meter unit)

Figure 12 Moment about the y-axis for the first and tallest buildings, at various distance x

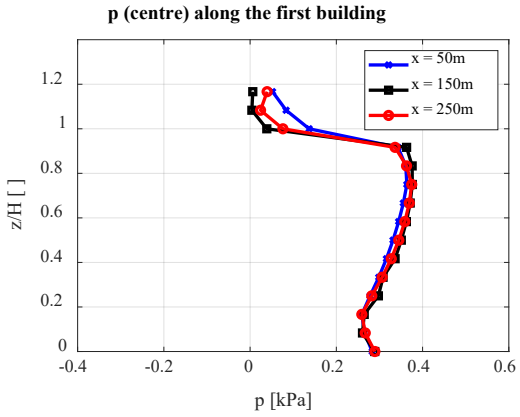


Figure 13 Pressure distribution (in the vertical direction) at the centreline of the first (Yellow) building at three different distances x = 50m, 150m, 250m. The vertical distance given in the y-axis is normalized by the building's height i.e. H = 30m

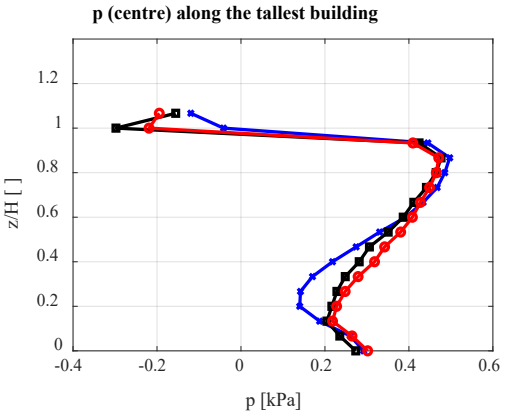


Figure 14 Pressure distribution (in the vertical direction) at the centreline of the tallest (Red) building at three different distances x = 50m, 150m, 250m. The vertical distance given in the y-axis is normalized by the building's height i.e. H = 75m

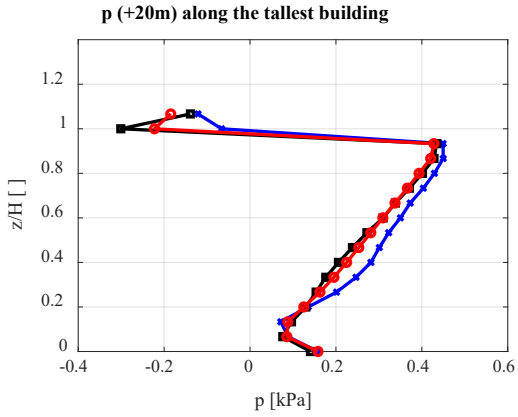


Figure 15 Pressure distribution (in the vertical direction) at the left-side (+20m from centreline) of the tallest (Red) building at three different distances x = 50m, 150m, 250m. The vertical distance given in the y-axis is normalized by the building's height i.e. 75m

The vertical pressure distribution 20 meters right of the centerline on the tallest (red) building, as shown in Figure 16, is analyzed for horizontal distances of x=50m, 150m, and 250m, with vertical distances normalized by the building's height of 75m. Maximum pressure values are $p_{\max}$ =0.415 *kPa* at z=70 m (x=250 m) and $p_{\max}$ =0.448 *kPa* at the same height (x=50 m), showing a 7.6% difference in magnitude at identical vertical positions. Both $p_{\max}$ values occur at z=70 m (normalized height: 70/75 ≈ 0.93), aligning with the left-side results, which suggests symmetry in high-pressure zones near the building's top. The larger percentage difference (7.6% vs. left-side 4.8%) indicates slightly greater sensitivity to horizontal spacing on the right side.

Minimum pressure values exhibit dramatic contrasts: $p_{\min}$ =0.088 *kPa* at z=5 m (x=250 m) and $p_{\min}$ =0.048 *kPa* at z=15 m (x=50 m), resulting in a

DOI: https://doi.org/10.11113/jurnalteknologi.v89.25538

58.8% magnitude difference and a 10m vertical positional gap. The 58.8% difference in $p_{\min}$ and 10m vertical shifts are far more pronounced than left-side results (17.7%, 5m), highlighting asymmetric wind effects. At x = 50m, the lower pressure (0.048*kPa*) occurs at a higher vertical position (right-side z = 15 m vs. left-side z = 10m), suggesting closer spacing amplifies suction forces on the right side. This asymmetry happens due to the position of the first building being slightly on the right side of the centreline of the tallest building.

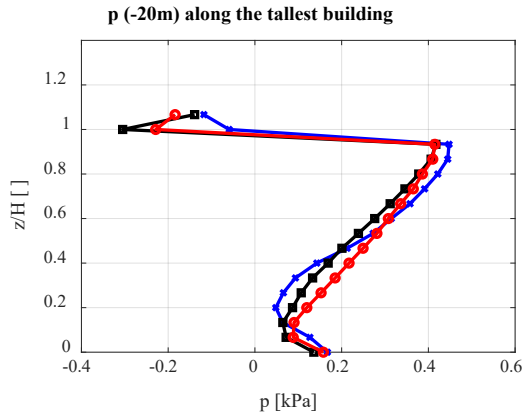


Figure 16 Pressure distribution (in the vertical direction) at the right-side (-20m from centreline) of the tallest (Red) building at three different distances x = 50m, 150m, 250m. The vertical distance given in the y-axis is normalized by the building's height i.e. 75m.

The study highlights three critical insights for urban wind engineering:

1. **Upper Building Stability**: High-pressure zones near building tops (*z>0.8H*) remain consistent across configurations, implying predictable wind loads for rooftop structures.

2. **Lower Region Vulnerability:** Minimum pressures at lower heights (*z<0.2H*) vary drastically with horizontal spacing, especially on the red building's right side, necessitating adaptive cladding and structural reinforcement in these zones.

3. **Asymmetric Wind Effects**: The first (yellow) building's off-center placement relative to the tallest (red) building exacerbates right-side suction forces, underscoring the importance of neighboring structure positioning in urban planning.

These findings advocate for façade-specific wind load assessments in dense urban layouts, prioritizing sensor deployment at lower heights and asymmetric reinforcement strategies. Future work should integrate 3D CFD modelling to quantify wake interactions and validate optimal spacing thresholds.

4.0 CONCLUSION

The present study demonstrates that inter-building spacing plays a decisive role in wind-induced pressures, velocity fields, and structural moments among adjacent high-rise buildings in dense urban environments, as systematically investigated using validated Reynolds-Averaged Navier-Stokes (RANS) simulations with a k-epsilon turbulence model. Mesh sensitivity analysis identified that a grid with approximately 1.7 million cells provides an effective balance between computational efficiency and accuracy, with finer meshes yielding diminishing returns. Both uniform and sheared atmospheric boundary layer inflows reveal that closely spaced buildings (e.g., 50 m) cause markedly increased wind loads and flow acceleration between structures, leading to amplified pressures and structural demands on downstream buildings, especially near ground level and along vulnerable façade regions. Vertical and lateral assessments of surface pressures highlight substantial sensitivity to spacing, particularly at building bases where suction forces and pressure fluctuations are most extreme, advocating for adaptive cladding and reinforcement strategies. The findings reinforce the importance of carefully considered building arrangement and façade-specific design in urban wind engineering, and recommend the ongoing development of advanced turbulence modeling and dynamic mesh adaptation for future studies involving multi-building CFD analysis under atmospheric boundary layer conditions.

The limitation of the present study is the computational power, where all simulations are conducted on a computer with 16 cores AMD Ryzen 9 processor, which limits the use of turbulence modelling to RANS model only, which is less accurate in predicting flow separation and eddy formation compared to LES model.

Future work would be to conduct comparative study on multiple RANS model for prediction on the standard CAARC tall building on multiple wind flow angle since the literature on this particular topic is scarce and therefore not many information or research has been done on this, to further study the loading variation on tall buildings.

Acknowledgement

The authors fully acknowledged Center for River and Coastal Engineering (CRCE) and Engineering Seismology and Earthquake Engineering Research (ESEER), Universiti Teknologi Malaysia, for the computational facilities used for running simulations.

DOI: https://doi.org/10.11113/jurnalteknologi.v89.25538

Conflicts of Interest

The authors declare that there is no conflict of interest regarding the publication of this paper.

Data availability

The data supporting the findings of this study are available from the corresponding author upon reasonable request.

Ethics declaration

Formal ethical approval was not obtained for this study. However, the authors confirm that the research was conducted in accordance with established ethical principles and good research practices, with due consideration given to participant rights, informed consent, confidentiality, and responsible data handling.

References

[1] Abu-Zidan, Y., Mendis, P., Gunawardena, T., Mohotti, D., & Fernando, S. (2022). Wind Design of Tall Buildings: The State of the Art. *Electronic Journal of Structural Engineering*, 22(1), 53–71. https://doi.org/10.56748/ejse.2233101

[2] Ashrith, T., & Sreenu, R. (2024). Wind Study on Isolated High Rise Building : A Computational Fluid Dynamic Approach. 45(1), 4994–5005.

[3] Blocken, B., Stathopoulos, T., van Beeck, J.P.A.J (2016) Pedestrian-level wind conditions around buildings: Review of wind-tunnel and CFD techniques and their accuracy for wind comfort assessment. *Building and Environment* vol. 100 (2016) pp 50-81.

[4] BS EN 1991-1-4:2005+A1:2010. Eurocode 1: Actions on structures – Part 1-4: General actions – Wind actions. British Standards Institution.

[5] Chen, J., Quan, Y., & Gu, M. (2020). Aerodynamic interference effects of a proposed super high-rise building on the aerodynamic forces and responses of an existing building. *Journal of Wind Engineering and Industrial Aerodynamics,* 206(June),104312. https://doi.org/10.1016/j.jweia.2020.104312

[6] H. Cui, M. Ma, J. Li, L. Yang, Z. Han and Q. Liu (2024) Integrated Impacts of Building Space Ratio and Wind Direction on Pedestrian-level Wind Environment around High-rise Buildings with Equilateral Triangle Arrangement. *Journal of Applied Fluid Mechanics*, Vol. 17, No. 9, pp. 2016-2027, 2024.

[7] Idrissi, A., El Mghari, H., & El Amraoui, R. (2025). CFD simulation advances in urban aerodynamics: Accuracy, validation, and high-rise building applications. *Results in Engineering*, 26(March), 105148. https://doi.org/10.1016/j.rineng.2025.105148

[8] Jayant, B., Rukhaiyar, A., Dahiya, K., & Raj, R. (2023). CFD Analysis for Wind Flow Characteristics of Varying Cross-Section Tall Building Using ANSYS. *Lecture Notes in Civil Engineering*, 285, 307–320. https://doi.org/10.1007/978-981-19-5077-3_25

[9] Li, Y., Li, C., Li, Q. S., Song, Q., Huang, X., & Li, Y. G. (2020). Aerodynamic performance of CAARC standard tall building model by various corner chamfers. *Journal of Wind Engineering and Industrial Aerodynamics*, 202(December 2019). https://doi.org/10.1016/j.jweia.2020.104197

[10] Li, Y., Song, Q., Li, C., Huang, X., & Zhang, Y. (2022). Reduction of wind loads on rectangular tall buildings with different taper ratios. *Journal of Building Engineering*, 45 (September 2021). https://doi.org/10.1016/j.jobe.2021.103588

[11] Li, Y., Zhu, Y., Chen, F. bin, & Li, Q. S. (2023). Aerodynamic loads of tapered tall buildings: Insights from wind tunnel test and CFD. Structures, 56 (April). https://doi.org/10.1016/j.istruc.2023.104975

[12] Liu, S., Pan, W., Zhang, H., Cheng, X., Long, Z., & Chen, Q. (2017). CFD simulations of wind distribution in an urban community with a full-scale geometrical model. *Building and Environment,* 117, 11–23. https://doi.org/10.1016/j.buildenv.2017.02.021

[13] Meddage, D. P. P., Mohotti, D., Wijesooriya, K., & Lee, C. K. (2024). Predicting Transient Wind Pressure Over A Tall Building Using Machine Learning. 20–21.

[14] Mittal, A. K., Ghosh, D., Behera, S., Siddiqui, I. A., & Dharmshaktu, D. S. (2013). Wind flow simulation in the vicinity of tall buildings through CFD. *Proceedings of the 8th Asia-Pacific Conference on Wind Engineering*, APCWE 2013, 2012, 682–690. https://doi.org/10.3850/978-981-07-8012-8_329

[15] Mon Soe, T., Khaing, Y., & Thein, K. K. (2019). Study on Wind Flow Behaviours of High Rise Buildings with CFD Simulation. Technology, and Sciences (ASRJETS) *American Scientific Research Journal for Engineering,* 54(1), 111–121. http://asrjetsjournal.org/

[16] Potsis, T., Tominaga, Y., Stathopoulos, T. (2023). Computational Wind Engineering: 30 years of research progress in building structures and environment. Journal of Wind Engineering and Industrial Aerodynamics, 234, 2023, 105346.

[17] Reiter, S. (2008). Validation Process for CFD Simulations of Wind Around Buildings-2008. *European Built Environment CAE Conference*, 1, 1–18.

[18] Shirzadi, M., Mirzael, P. A., Tominaga, Y. (2020). CFD analysis of cross-ventilation flow in a group of generic buildings: Comparison between steady RANS, LES and wind tunnel experiment. Building Simulation, 2020, Vol. 13 No. 6, 1353-1372.

[19] Tominaga, Y., Stathopoulos, T. (2010). Numerical simulation of dispersion around an isolated cubic building: Model evaluation of RANS and LES. Journal of Building and Environment, Vol. 45 (2010) 2231-2239.

[20] Wilcox, D. C. (1993). Comparison of Two-Equation Turbulence Models for Boundary Layers with Pressure Gradient. AIAA Journal, Vol. 31, No. 8, 1993, pp. 1414-1421.